

Structure of GaAs($\bar{1}\bar{1}\bar{1}$) under Ga-rich conditions: A $\sqrt{19}\times\sqrt{19}$ reconstruction model

Hiroaki Koga

Research Center for Integrated Quantum Electronics (RCIQE), Hokkaido University, North 13 West 8, Sapporo 060-8628, Japan

(Received 6 May 2010; revised manuscript received 15 July 2010; published 1 September 2010)

A GaAs($\bar{1}\bar{1}\bar{1}$) $\sqrt{19}\times\sqrt{19}$ reconstruction model that is almost consistent with the electron-counting (EC) rule was developed. This model differs from earlier hexagonal-ring models by three As atoms surrounding the ring and an As atom filling its center. First-principles calculations found that the model is more stable than the earlier non-EC models and is consistent with the hexagonal-ring patterns observed by scanning-tunneling microscopy. The applicability of the EC rule was thus reconfirmed. The stacking fault energy of the reconstruction was also calculated and found to be much higher than that of the 2×2 reconstruction. The Ga-rich conditions that stabilize the $\sqrt{19}\times\sqrt{19}$ reconstruction are therefore expected to suppress stacking faults in GaAs.

DOI: [10.1103/PhysRevB.82.113301](https://doi.org/10.1103/PhysRevB.82.113301)

PACS number(s): 68.35.B-, 61.46.Km, 61.72.Nn, 61.72.uj

Gallium arsenide and related III-V semiconductors continue to occupy a prominent position in solid-state physics. Currently, these materials are studied in various forms such as quantum dots,¹ nanowires,² and diluted magnetic semiconductors³ because of broad interest in quantum electronics and spintronics. Because such studies typically begin with the growth of films and nanostructures, it is very important to understand the structure of GaAs surfaces and its effect on growth and morphology.

The structure of III-V semiconductor surfaces is mostly explained in terms of the electron-counting (EC) rule,^{4,5} which states that a stable structure has precisely enough electrons to fill anionic dangling bonds and leave cationic ones empty (EC model). However, the $\sqrt{19}\times\sqrt{19}$ reconstruction,⁶ one of the two major phases of GaAs($\bar{1}\bar{1}\bar{1}$), is known to violate this rule. Because the surface region of this reconstruction expands $0.75\times 19=14.25$ electrons to splice itself onto the bulk at a (111)/($\bar{1}\bar{1}\bar{1}$) interface, it always has a nonintegral number of excess electrons (ν). To complete the physics of III-V surfaces, it is necessary to clarify the structure of this reconstruction and reconcile it with the rule.

The $\sqrt{19}\times\sqrt{19}$ reconstruction is also of interest in connection with stacking faults in GaAs nanowires. III-V semiconductor nanowires have the potential to enhance the current Si-based microelectronics by their superior transport and optical properties because they can be grown coherently on a Si substrate.⁷⁻¹⁰ The prevalence of stacking faults¹¹ (twin planes) parallel to the ($\bar{1}\bar{1}\bar{1}$) growth facet, however, could impede their applications. Although the stacking faults are usually discussed in terms of the nanowire's large lateral facets,¹² the faults are not peculiar to the nanowires but are common to GaAs and related ($\bar{1}\bar{1}\bar{1}$) films. Interestingly, the faults become less prevalent in films grown under the Ga-rich conditions that stabilize the $\sqrt{19}\times\sqrt{19}$ reconstruction.¹³⁻¹⁵ A similar trend is found for the initial structures of GaAs nanowires grown by using masks (selective-area growth).¹⁶ The reconstruction may thus be a key to controlling stacking faults in GaAs films and nanowires.

However, our understanding of the $\sqrt{19}\times\sqrt{19}$ reconstruction is rather unsatisfactory. Among the models of this recon-

struction, three are consistent with the hexagonal-ring patterns observed by scanning-tunneling microscopy (STM).⁶ The early model [Fig. 1(a)] by Biegelsen *et al.*⁶ ($\nu=3.75$) features six twofold coordinated Ga atoms buttressing a hexagonal ring. This structure is unlikely to be stable because it has too many dangling bonds due to the twofold-coordinated

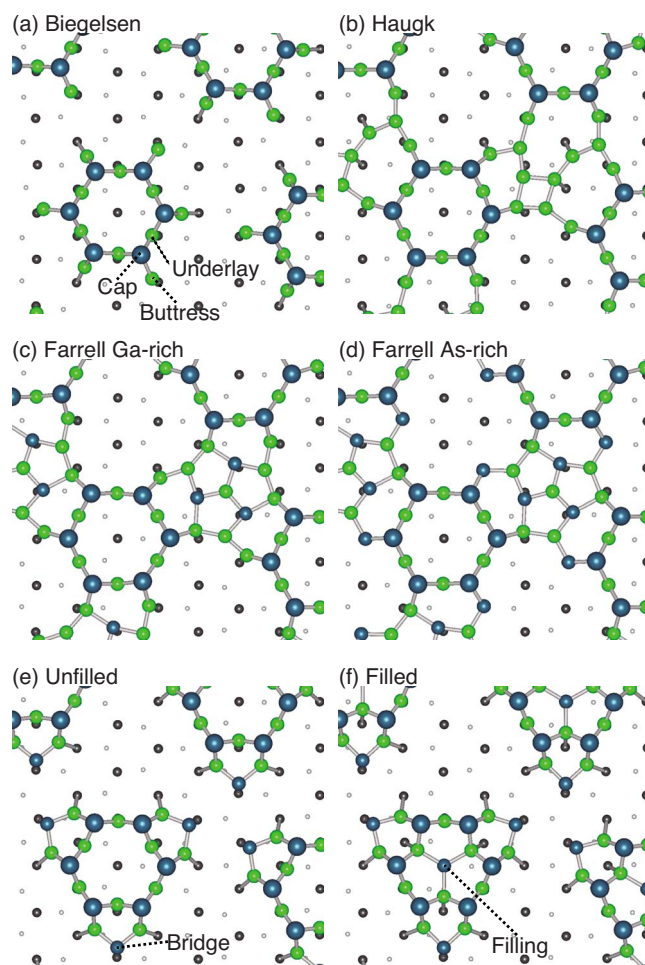


FIG. 1. (Color online) Hexagonal-ring models (plan view of optimized geometries); Ga and As denoted by green (light) and blue (dark) circles, respectively; upper atoms appear bigger.

atoms. Later models by Haugk *et al.*¹⁷ ($\nu=-2.25$) and Farrell *et al.*¹⁸ ($\nu=0.75$) resolve this by connecting the rings through a network of bonds [Figs. 1(b)–1(d)] but these models contradict the random distribution of rings observed during the 2×2 -to- $\sqrt{19}\times\sqrt{19}$ transition.¹⁹ Moreover, the stability of these models has not been verified from first principles; in fact, they turned out to be unstable in this investigation. A new model is therefore needed.

In this Brief Report, a $\sqrt{19}\times\sqrt{19}$ reconstruction model [Fig. 1(f)] with a nearly zero electron count is developed. First-principles calculations find this model to be more stable than earlier non-EC models, confirming the applicability of the EC rule. This greatly simplifies the physics of III-V surfaces. Then, a simulated STM image shows the model to be consistent with the observed hexagonal-ring patterns. Finally, we briefly discuss how the reconstruction may suppress stacking faults in GaAs.

The Biegelsen model [Fig. 1(a)] provides a good starting point because it is the simplest model of the hexagonal ring. The ring can be fortified by surrounding it with three As atoms, each bridging two buttressing Ga atoms and thus making them threefold coordinated [unfilled model, Fig. 1(e)]. This modification also reduces ν from 3.75 to 0.75. The same could be accomplished by using Ga bridges but the sp^2 rehybridization of the bridging Ga atom would conflict with that of its neighboring Ga atoms. Moreover, the bridging As atom is bonded to an As atom below, consistent with the presence of As-As bonds suggested by photoemission spectroscopy.^{20,21}

The electron count can be reduced further by placing an As atom at the center of the ring [filled model, Fig. 1(f)]. The new As atom, the As atom below it, and partially occupied Ga dangling bonds provide 5, 2, and 0.75 electrons, respectively, while eight electrons are required by the four bonds created by the filling. The electron count is thus reduced to -0.25 . Further, an EC model with $2\sqrt{19}\times 2\sqrt{19}$ periodicity can be constructed by combining an unfilled ring and three filled rings: the 0.75 excess electron of the former compensates for the deficiency of $0.25\times 3=0.75$ electron of the latter. This model represents a disordered $\sqrt{19}\times\sqrt{19}$ surface where one quarter of the filling As atoms are missing (missing model).

To determine the relative stability of the models, I have calculated optimized geometries and total energies within the generalized gradient approximation²² of density-functional theory^{23,24} (DFT) using a first-principles molecular-dynamics code called STATE.^{25–27} Norm-conserving pseudopotentials²⁸ and a plane-wave cut-off energy of 16 Ry were used. The surface was represented by an eight-layer periodic slab model. The back of the slab was terminated in pseudohydrogens (fictitious element 1.25), thus preventing unphysical electron transfer between sides.²⁹ The pseudohydrogen terminators as well as the bottom bilayer were frozen during geometrical optimization. The unit cells (k -point meshes) were 2×2 (4×4), $\sqrt{19}\times\sqrt{19}$ (2×2), and $2\sqrt{19}\times 2\sqrt{19}$ (1×1). For comparison, 2×2 Ga-atom, As-vacancy, and As-trimer models³⁰ were also calculated. The above conditions yielded well-converged energy differences (~ 3 meV/ 1×1). Moreover, the lattice constant and cohesive energy of GaAs [0.5653 nm (Ref. 31) and 3.34 eV/atom

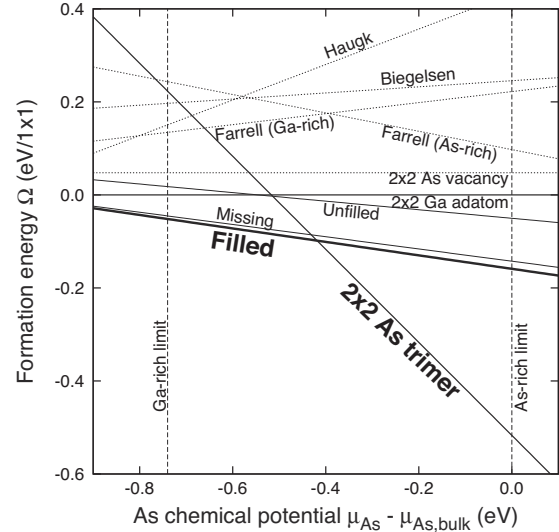


FIG. 2. Formation energy Ω of GaAs($\sqrt{19}\times\sqrt{19}$) reconstructions (relative to that of the Ga adatom model) versus As chemical potential (relative to bulk), $\mu_{\text{As}} - \mu_{\text{As,bulk}}$; range bounded by Ga- and As-rich limits.

(Ref. 32)] were well reproduced (0.5654 nm and 3.32 eV/atom).

The stability of a surface structure depends on chemical potentials μ_{Ga} and μ_{As} , and the structure with the lowest formation energy^{33,34}

$$\Omega = E - n_{\text{Ga}}\mu_{\text{Ga}} - n_{\text{As}}\mu_{\text{As}} \quad (1)$$

$$= E - n_{\text{Ga}}\varepsilon_{\text{GaAs}} + (n_{\text{Ga}} - n_{\text{As}})\mu_{\text{As}} \quad (2)$$

is realized, where E and n_{Ga} (n_{As}) are the total energy of the slab model and the number of Ga (As) atoms, respectively; we used the equilibrium condition $\varepsilon_{\text{GaAs}} = \mu_{\text{Ga}} + \mu_{\text{As}}$, where $\varepsilon_{\text{GaAs}}$ is the energy of GaAs. Because the chemical potentials cannot exceed their bulk levels, $\mu_{\text{As}} - \mu_{\text{As,bulk}}$ is restricted to the range $-\Delta H_f$ to 0, where $\Delta H_f = 0.74$ eV is the formation enthalpy of GaAs.^{35,36}

The calculated formation energies are plotted as a function of the As chemical potential in Fig. 2. The 2×2 As-trimer model is the most stable one under As-rich conditions, and the energy difference between the As-vacancy and Ga-atom models (3 meV/ \AA^2) is close to an earlier DFT result (2 meV/ \AA^2).^{30,37} Within the allowed range of chemical potentials, the earlier models (Biegelsen, Haugk, Farrell Ga rich and As rich) are higher in energy than the Ga-atom model and are thus unlikely candidates. In contrast, the unfilled model is much lower in energy than the earlier models and the filled model even lower. The filled model is more stable than the Ga-atom model in the relevant range and is also more stable than the 2×2 As-trimer model under Ga-rich conditions, consistent with the 2×2 -to- $\sqrt{19}\times\sqrt{19}$ transition.⁶

The filled model ($\nu=-0.25$) is also lower in energy than the missing model ($\nu=0$). The electron count of the filled model is practically zero given the large cell, and the additional transfer of a mere 0.75 electron per $2\sqrt{19}\times 2\sqrt{19}$ cell

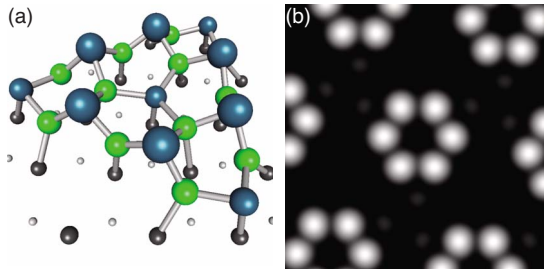


FIG. 3. (Color online) (a) Perspective view of filled ring. (b) Simulated occupied-state STM image of filled model obtained by integrating local density of states from valence band maximum to 1.8 eV below (cross section 0.11 nm above capping As atoms).

is apparently insufficient to make a dominant contribution. The $\sqrt{19} \times \sqrt{19}$ surface is therefore likely to be a surface without an energy gap, consistent with the small range of STM bias voltages where tunneling becomes unstable.⁶ The EC rule is thus contradicted but not significantly. To recover the applicability of the EC rule, it suffices to regard models with a nearly zero electron count per area as EC models.

Optimized geometries of hexagonal-ring models are shown in Fig. 1 (see Ref. 38 for coordinates). Owing to p^3 rehybridization, capping As atoms buckle toward vacuum, causing the hexagonal ring to shrink [see also Fig. 3(a)]. As a result, the diameters of the ring in the Biegelsen, unfilled, and filled models (0.812 nm, 0.826 nm, and 0.812 nm, respectively) were much smaller than that (0.923 nm) expected from the lattice constant. In the Haugk and Farrell Ga-rich and As-rich models, in contrast, larger diameters (0.856 nm on average, 0.869 nm, and 0.887 nm, respectively) were found because the connection between rings prevented them from shrinking. Connected models are thus at a disadvantage in terms of relaxation.

A simulated occupied-state STM image of the filled model is shown in Fig. 3(b). The brightest spots are located at capping As atoms and form hexagonal-ring patterns. The As atoms surrounding the ring give rise to much weaker spots, lying 0.12 nm below the capping ones. Moreover, the ring appears hollow because the filling As atom at the center is fourfold coordinated [Fig. 3(a)] and has no dangling bonds. The filled model is thus consistent with the hollow hexagonal-ring patterns observed by STM.⁶

We now discuss the relationship between reconstructions and stacking faults. Suppose that a stacking fault is introduced when a new layer forms in the faulted state on the $(\bar{1}\bar{1}\bar{1})$ growth surface and becomes buried as GaAs grows layer by layer. Because a layer needs to be stabilized by reconstruction, the probability of having a faulted layer is linked to that of a reconstruction phase forming on that layer. Now, an $(m \times n)$ surface phase occurs with a probability proportional to $\exp[-(m \times n)\Omega/k_B T]$, where Ω is the formation energy per 1×1 , k_B the Boltzmann constant, T temperature.³³ The probability of having a faulted layer is therefore $\exp(-E_{SF}/k_B T)$, where E_{SF} is the energy difference per reconstruction cell between models with and without a stacking fault immediately below the surface (Fig. 4). The

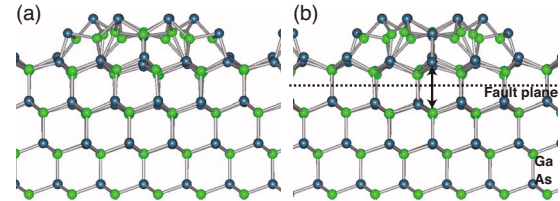


FIG. 4. (Color online) (a) Unfaulted and (b) faulted configurations of filled model (side view); double arrow denotes anion-cation interaction.

calculated values of E_{SF} are 0.107 eV and 0.304 eV for the 2×2 As-trimer and $\sqrt{19} \times \sqrt{19}$ filled-ring models, respectively. At relevant temperatures (500–800 °C), the probability will be much higher for 2×2 (20–30 %) than $\sqrt{19} \times \sqrt{19}$ (1–4 %). This is qualitatively consistent with the experimentally observed trends.^{13–16} Although this simple argument neglects detailed growth processes and the distinction between nanowires and films, it illustrates how the reconstruction may suppress stacking faults in GaAs.

It is interesting to reflect on the result that the stacking fault energy per area was actually smaller with the filled hexagonal-ring model. The surface As layer below the filled rings is more ionic than that below the As trimers because a smaller proportion of As atoms have a homopolar bond to an As atom above (4/19 vs 3/4). More ionicity makes stacking faults less unfavorable because of the electrostatic interaction between the anions of the faulted layer and the cations below [Fig. 4(b)]. Yet, the $\sqrt{19} \times \sqrt{19}$ reconstruction showed a higher E_{SF} because of its large reconstruction cell. To generalize, growth conditions that stabilize larger reconstructions are more likely to suppress stacking faults.

In summary, a GaAs $(\bar{1}\bar{1}\bar{1})$ $\sqrt{19} \times \sqrt{19}$ hexagonal-ring reconstruction model has been developed so that it may be consistent with the EC rule. This model was obtained by surrounding the ring by three As atoms and filling its center with an As atom. DFT calculations showed that this filled model is more stable than 2×2 models under Ga-rich conditions, as is consistent with the 2×2 -to- $\sqrt{19} \times \sqrt{19}$ transition. Earlier non-EC models (Biegelsen, Haugk, and Farrell), on the other hand, were found to be inconsistent with the transition. The filled model has a nearly zero electron count per 1×1 , so the applicability of the EC rule can be recovered by considering such models as EC models. A simulated STM image showed that the model is consistent with the hollow hexagonal-ring patterns observed by STM. DFT calculations also found that the stacking fault energy of the $\sqrt{19} \times \sqrt{19}$ filled-ring model is higher than that of the 2×2 As-trimer model. The Ga-rich conditions that stabilize the $\sqrt{19} \times \sqrt{19}$ reconstruction are therefore expected to suppress stacking faults in GaAs.

The author thanks K. Hiruma and H. Yoshida for sharing their insights about nanowire growth experiments. Some of the DFT calculations were run on the computers of the Information Technology Center, the University of Tokyo. This work was in part supported by JSPS under Grant No. 21860001.

- ¹S. M. Reimann and M. Manninen, *Rev. Mod. Phys.* **74**, 1283 (2002).
- ²S. A. Dayeh, C. Soci, X.-Y. Bao, and D. Wang, *Nano Today* **4**, 347 (2009).
- ³T. Jungwirth, J. Sinove, J. Mašek, J. Kučera, and A. H. MacDonald, *Rev. Mod. Phys.* **78**, 809 (2006).
- ⁴M. D. Pashley, *Phys. Rev. B* **40**, 10481 (1989).
- ⁵The physics behind the EC rule is electron transfer from high-lying cationic dangling-bond levels to low-lying anionic ones, and the maximization of the resulting energy gain due to sp^2 (p^3) rehybridization of threefold-coordinated cations (anions). The rehybridization raises (lowers) dangling-bond levels, opening an energy gap, and causes the cations to adopt planar (pyramidal) bonding geometry. The number of excess electrons (ν) is counted by adding three (five) electrons per cation (anion) and subtracting two per two-center bond, two per anionic dangling bond, and the number required to splice the surface region onto the bulk.
- ⁶D. K. Biegelsen, R. D. Bringans, J. E. Northrup, and L.-E. Swartz, *Phys. Rev. Lett.* **65**, 452 (1990).
- ⁷T. Mårtensson, C. P. T. Svensson, B. A. Wacaser, M. W. Larsson, W. Seifert, K. Deppert, A. Gustafsson, L. R. Wallenberg, and L. Samuelson, *Nano Lett.* **4**, 1987 (2004).
- ⁸K. Tomioka, J. Motohisa, S. Hara, and T. Fukui, *Nano Lett.* **8**, 3475 (2008).
- ⁹K. Tomioka, Y. Kobayashi, J. Motohisa, S. Hara, and T. Fukui, *Nanotechnology* **20**, 145302 (2009).
- ¹⁰H. Koga, *Phys. Rev. B* **80**, 245302 (2009).
- ¹¹M. Koguchi, H. Kakibayashi, M. Yasawa, K. Hiruma, and T. Katsuyama, *Jpn. J. Appl. Phys., Part 1* **31**, 2061 (1992).
- ¹²T. Akiyama, K. Nakamura, and T. Ito, *Phys. Rev. B* **73**, 235308 (2006).
- ¹³P. Chen, K. C. Rajkumar, and A. Madhukar, *Appl. Phys. Lett.* **58**, 1771 (1991).
- ¹⁴Y. Park, M. J. Cich, R. Zhao, P. Specht, E. R. Weber, E. Stach, and S. Nozaki, *J. Vac. Sci. Technol. B* **18**, 1566 (2000).
- ¹⁵S. Naritsuka, S. Matsuoka, T. Kondo, K. Saitoh, T. Suzuki, Y. Yamamoto, and T. Maruyama, *J. Cryst. Growth* **301-302**, 42 (2007).
- ¹⁶H. Yoshida, K. Ikejiri, T. Sato, S. Hara, K. Hiruma, J. Motohisa, and T. Fukui, *J. Cryst. Growth* **312**, 52 (2009).
- ¹⁷M. Haugk, J. Elsner, M. Sternberg, and T. Frauenheim, *J. Phys.: Condens. Matter* **10**, 4523 (1998).
- ¹⁸H. H. Farrell, J. Lu, B. D. Schultz, A. B. Denison, and C. J. Palmstrøm, *J. Vac. Sci. Technol. B* **19**, 1597 (2001).
- ¹⁹J. M. C. Thornton, D. A. Woolf, and P. Weightman, *Appl. Surf. Sci.* **123-124**, 115 (1998).
- ²⁰K. Nakamura, T. Mano, M. Oshima, H. W. Yeom, and K. Ono, *J. Appl. Phys.* **101**, 043516 (2007).
- ²¹H. H. Farrell, B. D. Schultz, and C. J. Palmstrøm, *J. Appl. Phys.* **105**, 056106 (2009).
- ²²J. P. Perdew, K. Burke, and M. Ernzerhof, *Phys. Rev. Lett.* **77**, 3865 (1996).
- ²³P. Hohenberg and W. Kohn, *Phys. Rev.* **136**, B864 (1964).
- ²⁴W. Kohn and L. J. Sham, *Phys. Rev.* **140**, A1133 (1965).
- ²⁵Y. Morikawa, H. Ishii, and K. Seki, *Phys. Rev. B* **69**, 041403(R) (2004).
- ²⁶I. Hamada and Y. Morikawa, *J. Phys. Chem. C* **112**, 10889 (2008).
- ²⁷S. Yanagisawa, K. Lee, and Y. Morikawa, *J. Chem. Phys.* **128**, 244704 (2008).
- ²⁸N. Troullier and J. L. Martins, *Phys. Rev. B* **43**, 1993 (1991).
- ²⁹K. Shiraishi, *J. Phys. Soc. Jpn.* **59**, 3455 (1990).
- ³⁰N. Moll, A. Kley, E. Pehlke, and M. Scheffler, *Phys. Rev. B* **54**, 8844 (1996).
- ³¹G. Giesecke and H. Pfister, *Acta Crystallogr.* **11**, 369 (1958).
- ³²E. Kaxiras, *Atomic and Electronic Structure of Solids* (Cambridge University Press, Cambridge, 2003), p. 199.
- ³³F. Bechstedt, *Principles of Surface Physics* (Springer-Verlag, Berlin, 2003), pp. 67–74.
- ³⁴The free energy of a slab is replaced by its total energy because vibrational contributions mostly cancel out for energy differences between similar structures (Ref. 33).
- ³⁵*CRC Handbook of Chemistry and Physics*, 67th ed., edited by R. C. West (CRC, Boca Raton, FL, 1986).
- ³⁶If we use the calculated formation energy of GaAs, the Ga-rich limit in Fig. 2 would be -0.82 eV. As can be seen from the figure, this would not affect the present conclusions.
- ³⁷The As bulk level in Fig. 9 of Ref. 30 appears to be shifted to the left compared to the present one. This is probably because Ref. 30 uses the local-density approximation, which overestimates binding energies.
- ³⁸See supplementary material at <http://link.aps.org/supplemental/10.1103/PhysRevB.82.113301> for coordinates.